Neurobiology of Aging 36 (2015) 2869–2876

Contents lists available at ScienceDirect

Neurobiology of Aging

journal homepage: www.elsevier.com/locate/neuaging

Mitochondrial decline precedes phenotype development in the complement factor H mouse model of retinal degeneration but can be corrected by near infrared light

Karin C. Calaza [a,b], Jaimie Hoh Kam [b], Chris Hogg [c], Glen Jeffery [b,*]

[a] Program of Neurosciences, Institute of Biology, Federal Fluminense University, Rio de Janeiro, Brazil
[b] Institute of Ophthalmology University College London, London, UK
[c] Moorfields Eye Hospital, London, UK

ARTICLE INFO

Article history:
Received 9 January 2015
Received in revised form 2 June 2015
Accepted 5 June 2015
Available online 15 June 2015

Keywords:
670 nm
Aging
Retina
AMD
ATP

ABSTRACT

Mitochondria produce adenosine triphosphate (ATP), critical for cellular metabolism. ATP declines with age, which is associated with inflammation. Here, we measure retinal and brain ATP in normal C57BL/6 and complement factor H knockout mice ($Cfh^{-/-}$), which are proposed as a model of age-related macular degeneration. We show a significant premature 30% decline in retinal ATP in $Cfh^{-/-}$ mice and a subsequent shift in expression of a heat shock protein that is predominantly mitochondrial (Hsp60). Changes in Hsp60 are associated with stress and neuroprotection. We find no differences in brain ATP between C57BL/6 and $Cfh^{-/-}$ mice. Near infrared (NIR) increases ATP and reduces inflammation. ATP decline in $Cfh^{-/-}$ mice was corrected with NIR which also shifted Hsp60 labeling patterns. ATP decline in $Cfh^{-/-}$ mice occurs before inflammation becomes established and photoreceptor loss occurs and may relate to disease etiology. However, ATP levels were corrected with NIR. In summary, we provide evidence for a mitochondrial basis for this disease in mice and correct this with simple light exposure known to improve mitochondrial function.

1. Introduction

The outer retina has the greatest metabolic demand in the body which is reflected in the high concentration of mitochondria in photoreceptors and their adenosine triphosphate (ATP) production that is critical for cellular metabolism (Yu and Cringle, 2001). With aging, mitochondrial (mt) DNA harbor an increased number of mutations and ATP production declines, while proinflammatory reactive oxygen species production increases (Archer, 2013; Balaban et al., 2005; Gkotsi et al., 2014). This forms the basis of the mitochondrial theory of aging originally proposed by Harman (Harman, 1972; Lane, 2005). A hallmark of retinal aging is progressive inflammation and extracellular deposition including that of proinflammatory amyloid beta (Aβ) on photoreceptor outer segments and Bruch's membrane. This is associated with progressive outer retinal cell loss (Hoh Kam et al., 2010, 2013). Even in normal aged eyes there is a 30% loss of photoreceptors over life in man and rodent (Cunea and Jeffery, 2007; Curcio, 2001).

Compromised mitochondrial function has been implicated in age-related macular degeneration (AMD) (Barot et al., 2011; Jarrett et al., 2008) but this has not been explored. AMD may be viewed as an advanced form of aging that will increase in incidence as life expectancy extends (AREDS2 Research Group et al., 2012). In half of the cases there is further complication of an association with compromised immunity due to polymorphisms of the complement system (Edwards et al., 2005; Haines et al., 2005) that may amplify inflammatory responses, increasing the rate of cell loss.

Here, we test directly the link between aging, retinal ATP, and polymorphisms of the complement system by examining ATP levels in normal aging eyes and those of complement factor H knockout mice ($Cfh^{-/-}$) that have been proposed as a murine AMD model (Coffey et al., 2007). We reveal premature ATP decline in $Cfh^{-/-}$ retinae and changes in patterns of labeling for heat shock protein 60 (Hsp60). Hsp60 is predominately mitochondrial. Heat shock proteins are a family of proteins expressed during stress, and Hsp60 chaperons correct protein folding and the replication and transmission of mtDNA. Hence, stress associated with inflammation may be reflected by changing Hsp60 patterns (Brocchieri and Karlin, 2000; Cappello et al., 2008; Kaufman et al., 2003; Ostermann et al., 1989; Saibil, 2013).

* Corresponding author at: Institute of Ophthalmology, University College London, Bath St., London EC1V 9EL, UK. Tel.: +442076086837; fax: +442076086909.
E-mail address: g.jeffery@ucl.ac.uk (G. Jeffery).

0197-4580/
http://dx.doi.org/10.1016/j.neurobiolaging.2015.06.010

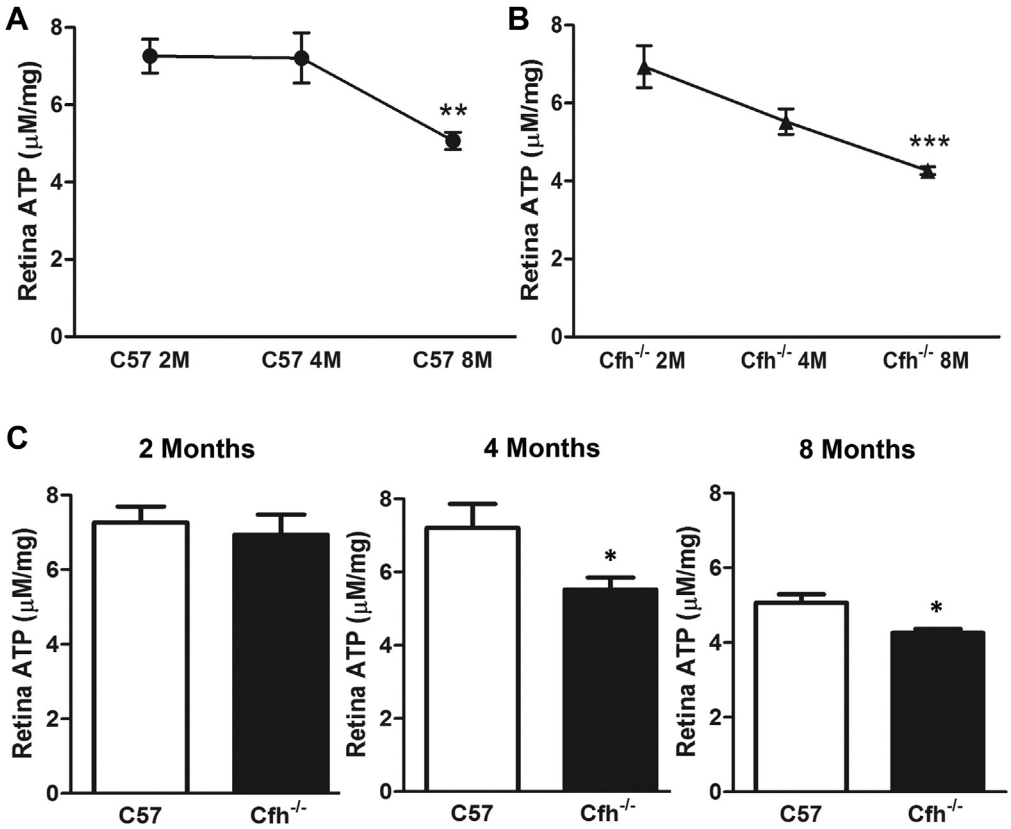

Fig. 1. (A) ATP levels in the retinae of C57BL/6 mice at 2 months, 4 months, and 8 months. There were no differences between 2 and 4 months. Differences were statistically significant between 2 and 8 months. (B) ATP levels in the retinae of *Cfh*$^{-/-}$ mice at 2 months, 4 months, and 8 months. There was a decline between 2 and 4 months that was not significant and a significant decline between 2 and 8 months. (C) Comparisons between levels of ATP in C57BL/6 and *Cfh*$^{-/-}$ at 2 months, 4 months, and 8 months. Levels between genotypes were similar at 2 months. However, at 4 months ATP levels in *Cfh*$^{-/-}$ declined significantly by comparison with C57BL/6. By 8 months, ATP levels declined in both groups but differences between the genotypes remained statistically significant being lower in *Cfh*$^{-/-}$. Unit of measurement is μM/mg tissue. Statistical tests were analysis of variance and Student *t* test. Levels of statistical significance: $^{*}p < 0.05$, $^{**}p < 0.01$, $^{***}p < 0.001$. Abbreviations: ATP, adenosine triphosphate; M, months.

ATP levels in the retina and brain can be increased by near infrared light at 670 nm (Gkotsi et al., 2014) as it is absorbed by cytochrome c oxidase (COX) in the mitochondrial respiratory chain (Griffiths and Wharton, 1961; Szundi et al., 2001; Wilson and Greenwood, 1970), significantly increasing its expression at both the protein and RNA levels (Begum et al., 2013). Near infrared light has also been widely used to reduce the impact of aging and experimental pathology and is effective where insult impacts on mitochondrial function (Fitzgerald et al., 2013). Furthermore, improvements induced by these wavelengths have been shown to increase ATP, reduce inflammation, and extend life span in flies where they also improve aged mobility (Begum et al., 2015). Here, we use 670-nm light to correct the premature ATP decline found in aged *Cfh*$^{-/-}$ mice.

2. Methods

Normal C57BL/6 mice and *Cfh*$^{-/-}$ on the same background were used at 2 (N = 10 per group), 4 (N = 10 per group), and 8 (N = 24 per group) months of age. All were housed in the same facility under standard conditions. For ATP measurements, mice were killed by cervical dislocation followed by immediate decapitation into iced Krebs solution. The eyes were removed and the retinae dissected out in the same solution in <30 seconds. The brains were rapidly removed from the skull, chilled, and macerated in cold 2.5% trichloroacetic acid (TCA). Both tissues were then rapidly frozen in 2.5% TCA on dry ice. Tissues were homogenized using a sonicator and centrifuged at 13,000 rpm for 10 minutes at 4 °C. The supernatant was collected and kept on ice. The 2.5% TCA of the supernatant was neutralized with 1 mol/L Tris-acetate buffer (pH 7.75; final concentration of TCA was 0.0625%) and 100 μL of the neutralized solution was added to an equal volume of luciferin (1 mM)-luciferase (100 μg/mL) in luciferase buffer (25-mM Tris-acetate, pH 7.75; 2-mM EDTA, 50-mM dithiothreitol, 1.5-mg/mL bovine serum albumin, 20-mM magnesium acetate) and the ATP levels were measured using the Orion microplate luminometer (Berthold Detection Systems GmbH). The data were then normalized by tissue weight.

Mouse eyes were also immune-stained for the mitochondrial Hsp60. Here, eyes were enucleated after cervical dislocation and placed in 4% paraformaldehyde in phosphate buffer (PBS, pH 7.2) for 1 hour. They were then washed repeatedly with PBS, the anterior chamber and lens were removed and the eye cup then placed in 30% sucrose in PBS overnight before being embedded in optimum cutting temperature. Retinal cryosections were cut at 10 μm and mounted onto superfrost slides. For immunohistochemistry, 5 mice were used for each age evaluated.

In addition, 12 *Cfh*$^{-/-}$ mice were used for 670-nm light exposure experiments; 6 were 670 nm light exposed and 6 were controls. Here, both groups of animals had their heads shaved so as to increase potential light exposure to the brain and were held at 10 cm in front of a 670-nm light source irradiating at 40 mW/cm^2 for 90 seconds daily for 5 days. Controls were held without light exposure. All mice were culled after the last exposure of the experimental group and their retinae and brains removed rapidly for ATP as previously mentioned. In previous unpublished experiments, we have found that white light alone has no impact on the metrics used here.

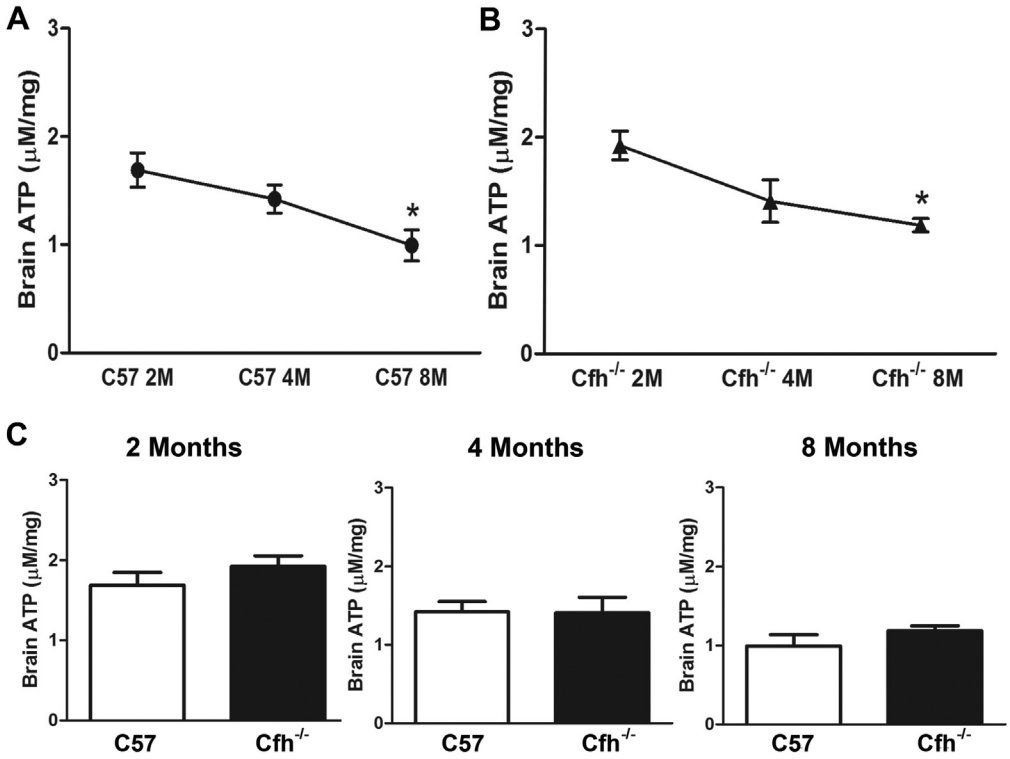

Fig. 2. (A) ATP levels in the brains of C57BL/6 mice at 2 months, 4 months, and 8 months. ATP levels declined approximately linearly with age and were significantly different between 2 and 8 months. (B) ATP levels in the brains of *Cfh*$^{-/-}$ mice at 2 months, 4 months, and 8 months. Patterns of decline and statistical significance were similar to C57BL/6 in A. (C) Comparisons of ATP levels in the brains of 2 months, 4 months, and 8 months C57BL/6 and *Cfh*$^{-/-}$ mice. There was a gradual decline in levels with age reflecting patterns in A and B. However, there were no differences in ATP levels in the brain between the 2 groups of mice. Unit of measurement is μM/mg tissue. Statistical tests were analysis of variance and Student *t* test. Levels of statistical significance: $^{*}p < 0.05$. Abbreviations: ATP, adenosine triphosphate; M, months.

Cryosections were washed in PBS (0.1 M) for 5 minutes, blocked with 5% normal donkey serum in 0.3% triton X-100 in PBS for 1 hour. Then, sections were incubated with a rabbit polyclonal Hsp60 antibody (1:200; Abcam). Subsequently, sections were washed in PBS and incubated with an Alexa-Fluor donkey anti-rabbit conjugated with 488 (1:1000, Invitrogen, Paisley, UK) with 2% normal donkey serum in 0.3% triton X-100 in PBS for 1 hour. After several washes with PBS, sections were incubated with 4′,6-diamidino-2-phenylindole (1:5000, Sigma Aldrich, Dorset, UK) for 1 minute for nuclei staining followed with several washes with PBS and Tris-buffered saline. Slides were mounted with Vectashield (Vector Laboratories, Peterborough, UK) and coverslipped.

For Western blots, eyes were dissected on ice and the retina and retinal pigmented epithelium choroidal tissues were snap-frozen in liquid nitrogen. Protein was then extracted by homogenizing the samples in 2% sodium dodecyl sulfate with protease inhibitor cocktail (Roche diagnostics) and centrifuged at 13,000*g*. The supernatant was transferred to a new microcentrifuge tube. Protein concentration was measured with an absorbance of 595 nm, and bovine serum albumin was used as a standard protein concentration. Proteins were separated by a 10% sodium dodecyl sulfate-polyacrylamide gel electrophoresis and electrophoretically transferred onto nitrocellulose membrane. The nitrocellulose membrane was pretreated with 5% nonfat dried milk in 1-M PBS (pH 7.4) for 2 hours and incubated overnight at 4 °C with a rabbit polyclonal antibody to Hsp60 (1:500, Abcam, UK) followed by several washes in 0.05% Tween-20 in 1-M PBS. The membrane was then incubated with a goat anti-rabbit horseradish peroxidase conjugated (1:2000, Dako), for 1 hour. Immunoreactivity was visualized by exposing X-ray films to blots incubated with enhanced chemiluminescence reagent (SuperSignal West Dura, Thermo Scientific). Total protein profile was determined by staining blot with Ponceau S solution to check the transfer efficiency. Protein bands were then photographed and scanned. To obtain the loading control, the membrane was washed in 0.05% Tween-20 in 1-M PBS and stripped with guanidine hydrochloride (6M, pH 7.5) and then immunoblotted with a mouse monoclonal anti α-tubulin (1: 2000, Millipore) in the same way as previously mentioned. The absolute intensity of each band was then measured using Adobe Photoshop CS5 extended.

For analysis of immunostaining, fluorescence images were taken in JPEG format at ×400 using an Epi-fluorescence bright-field microscope. Images were montaged and the pixel intensity was recorded using Adobe Photoshop CS5 extended. The lasso tool was used to draw a line all the way around the area of interest, that is, inner plexiform layer (IPL), outer plexiform layer (OPL), and the inner segment.

For Western blot measurement of Hsp60, scanned images of the immunoblot was inverted to gray-scale format and the mean gray value was measured for each protein band by using the lasso tool to draw a line all the way around the edges of the band using Adobe Photoshop CS5 extended. The absolute intensity was calculated by multiplying the mean gray value and the pixel value. The protein bands were quantified and their ratios to alpha tubulin were calculated and plotted into graphs.

3. Results

3.1. ATP and mitochondria in aging retina and brain of C57BL/6 and Cfh$^{-/-}$

ATP was measured in the aging retina and brain. In the retina, ATP levels were very similar in C57BL/6 mice at 2 and 4 months of age but showed a significant reduction at 8 months (Fig. 1A). In the

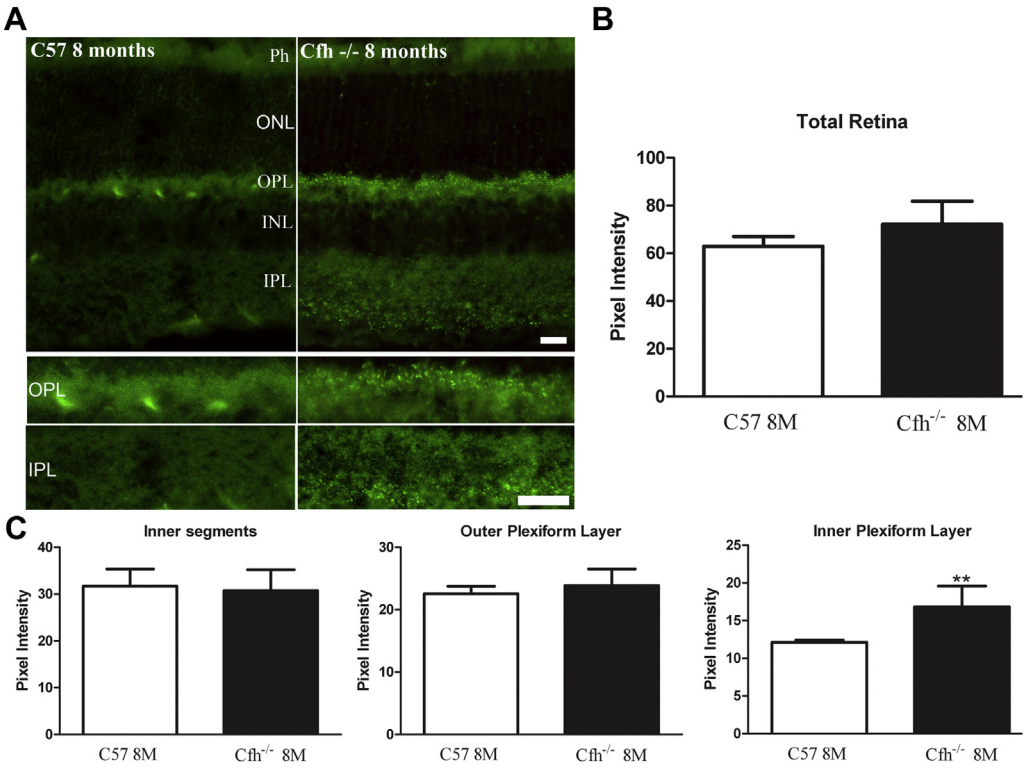

Fig. 3. Hsp60 labeling in 8-month-old C57BL/6 and Cfh^{-}/$^{-}$ mice. (A) Photomicrographs of retinal sections from 8-month-old C57BL/6 (left) and Cfh^{-}/$^{-}$ mice immunostained for Hsp60 (green). Labeling was present in diffuse patterns in the plexiform layers of C57BL/6 mice. However, in Cfh^{-}/$^{-}$ mice staining patterns are different and appears as punctate and focused. Label associated with the outer plexiform layers was very punctate and in many cases it was roughly circular or elongated in morphology corresponding to the morphology of individual mitochondria. This is seen more clearly in the panels at the bottom that are at a higher magnification. (B and C) Quantification of the fluorescence label. B is for total retina including all of the layers. C is the relative density for the inner segments, the outer plexiform layer, and the inner plexiform layer. The only significant difference between the 2 groups of mice is for the inner plexiform layer. However, the greatest distinction between the 2 groups of mice is in the distribution of the label rather than the absolute amount. Scale bars = 20 μm. Statistical analysis was done using Student *t* test. $^{**}p < 0.01$. Abbreviations: INL, inner nuclear layer; IPL, inner plexiform layer; ONL, outer nuclear layer; OPL, outer plexiform layer; Ph, photoreceptors. (For interpretation of the references to color in this figure legend, the reader is referred to the Web version of this article.)

Cfh$^{-/-}$ mice, there was an approximate 20% decline in ATP between 2 and 4 months that was not significant. But there was a significant decline at 8 months of approximately 40%, which was greater than that found over the same period in C57BL/6 mice (Fig. 1B) where the decline was <30%.

When retinal ATP levels were compared between the 2 mouse genotypes, no differences were found between C57BL/6 and *Cfh*$^{-/-}$ at 2 months of age. But at 4 months of age the 2 groups were significantly different with that in the *Cfh*$^{-/-}$ being approximately 20% lower than in C57BL/6 animals. At 8 months the significant difference was maintained with levels lower in *Cfh*$^{-/-}$ mice (Fig. 1C). Hence, retinal ATP decline is initiated relatively early in the *Cfh*$^{-/-}$ mouse and remain below levels found in C57BL/6 as the animals ages.

The changes found in ATP levels with aging in the brain were different from those in the eye. First, overall ATP levels at 2 months of age were lower in the brain in both genotypes by approximately 5 fold compared with levels in the retina, consistent with a previous comparison (Gkotsi et al., 2014). In both groups of animals, there was a gradual decline in ATP in the brain with age (Fig. 2A and B). There was a nonsignificant decline of around 20% between 2 and 4 months within both *Cfh*$^{-/-}$ and C57BL/6 and a decline of a similar proportion between 4 and 8 months. However, by 8 months of age both groups experienced statistically significant declines in ATP compared with that found at 2 months of age. There were no significant differences in ATP levels between the 2 mouse genotypes at any age (Fig. 2C). Hence, the premature decline in retinal ATP was confined to that organ.

ATP declines with age due to progressive mitochondrial dysfunction (Harman, 1972; Lopez-Otin et al., 2013) and mitochondrial dysfunction has been suggested as being associated with AMD (Nordgaard et al., 2008; Udar et al., 2009) and other age-related diseases (Archer, 2013). If correct, then it is possible that markers of mitochondrial stress in the retina may differ between C57BL/6 and *Cfh*$^{-/-}$ mice as they age. Hence, eyes from both groups were stained for Hsp60 (Fig. 3). Tissue was compared at 8 months between C57BL/6 and *Cfh*$^{-/-}$ when the decline in ATP was greatest in both groups. There were no obvious differences between the 2 mouse genotypes at 2 months of age in Hsp60 patterns with little or no staining present (data not shown), reflecting ATP data at this age. However, there were marked differences in these patterns between the 2 groups of mice at 8 months (Fig. 3). In 8-month-old C57BL/6 mice, label was relatively diffuse with concentration at the level of the inner segments, OPL and the IPL. A different pattern was seen in the 8-month-old *Cfh*$^{-/-}$ mice. Label was concentrated at the same locations but it was more punctate and condensed. This consistently appeared to be localized to individual structures that may correspond to separate mitochondria. This was less apparent in the photoreceptor inner segments, probably because of the high density of mitochondria here made identification of individual structure difficult. But it was marked in the region of the OPL where their terminals are located and in the IPL.

3.2. *Reversing ATP decline in* Cfh$^{-/-}$ *mice*

Six hundred seventy nanometer light corrects the age-related ATP decline in the retina and brain, probably because longer

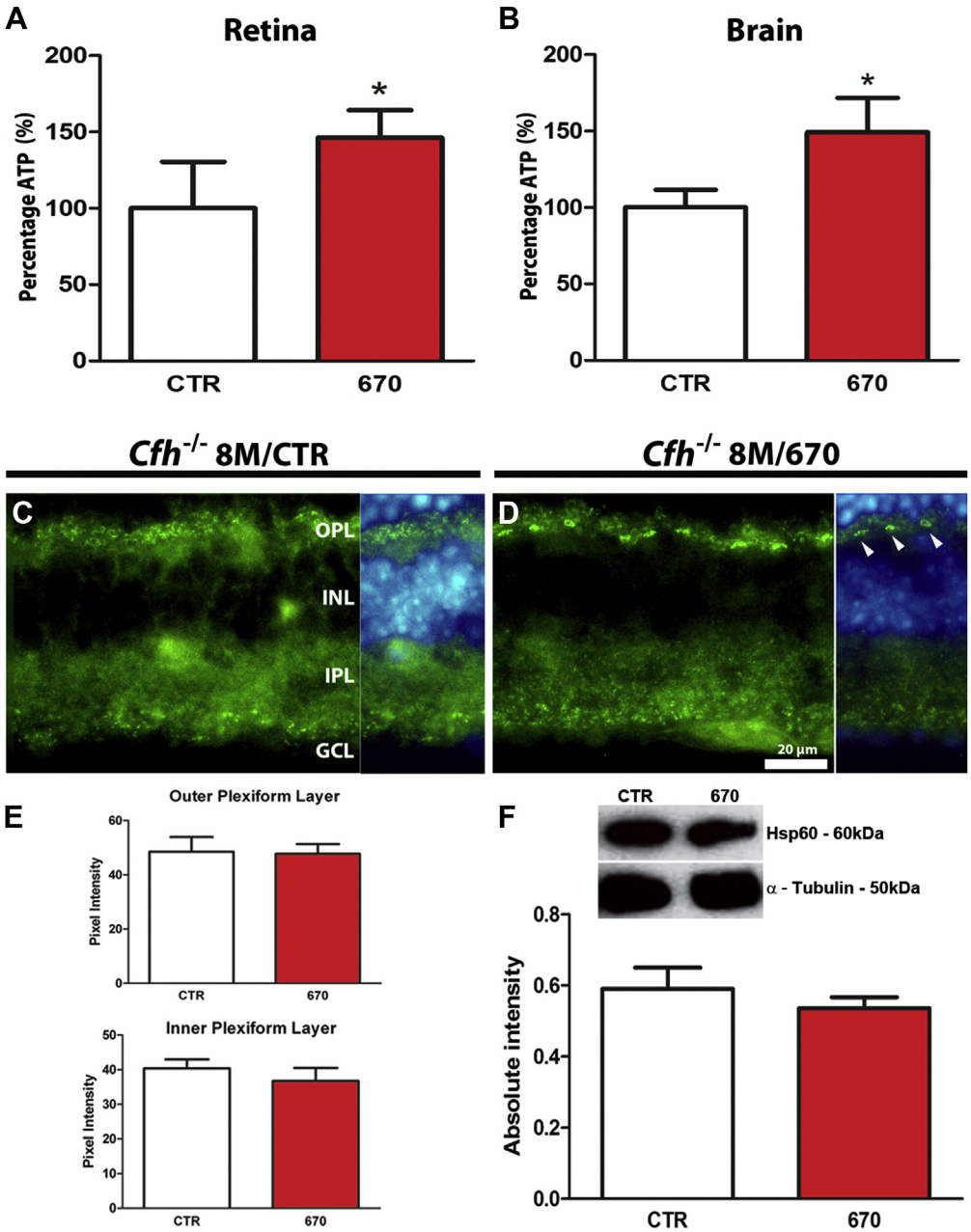

Fig. 4. (A) ATP levels in 8-month-old untreated *Cfh*$^{-/-}$ (CTR) mice and those exposed to 670-nm light (red) showing upregulation after light exposure. The untreated has been normalized to 100%. Six hundred seventy nanometer light exposure significantly increases ATP in aged *Cfh*$^{-/-}$ retinae. (B) The same data for brains of the same 2 groups of mice. Again 670-nm light significantly increases ATP levels. In both retina and brain the increase in ATP after light exposure is approximately 50%. (C) Patterns of Hsp60 label in untreated 8 months *Cfh*$^{-/-}$ mice (CTR). (D) Patterns of Hsp60 found after 670 nm exposure in 8-month-old *Cfh*$^{-/-}$. Staining patterns on the right side of C and D have been counter stained (blue) giving a clear indication of location. There are differences between Hsp60 staining in C and D. Noticeably, label was more focused and punctate in D. This is indicated with arrow heads on the right side. (E) When the total Hsp60 labels were measured from the section in the inner and outer plexiform layers, no significant differences were found. Plexiform layers were examined because differences were found here between genotypes in Fig. 3 (F). This was reflected in the Western blots where samples included the whole retina. Unit of measurement is µM/mg tissue. Statistical analysis was done using Student *t* test. $^{*}p < 0.05$. Abbreviations: CTR, control; GCL, ganglion cell layer; INL, inner nuclear layer; IPL, inner plexiform layer; OPL, outer plexiform layer. (For interpretation of the references to color in this figure legend, the reader is referred to the Web version of this article.)

wavelengths are absorbed by COX impacting on mitochondrial respiration (Gkotsi et al., 2014; Griffiths and Wharton, 1961; Szundi et al., 2001; Wilson and Greenwood, 1970). Furthermore, in normal aged C57BL/6 and *Cfh*$^{-/-}$ mice 670-nm light exposure increases mitochondrial membrane potentials and reduces age-related retinal inflammation (Begum et al., 2013; Kokkinopoulos et al., 2013).

As a premature decline in ATP is shown here to be a feature in the *Cfh*$^{-/-}$ mouse model, we employ 670-nm light exposure to determine if this can be corrected. Brief exposures of 670-nm light in 8-month-old *Cfh*$^{-/-}$ mice resulted in significantly elevated ATP with levels increased by approximately 50% over nontreated *Cfh*$^{-/-}$ mice in both the eye and the brain (Fig. 4A and B). Increases in the brain were due to the ability of these longer wavelengths to penetrate deeply, as shown previously in both mouse and rat brain (Fitzgerald et al., 2013; Gkotsi et al., 2014).

If there are improvements in ATP production then this may also be reflected in changes in Hsp60 expression. These patterns are

shown in Fig. 4C and D, again for 8-month-old *Cfh*$^{-/-}$ for 670-nm light treated and untreated mice. There are differences between the light treated and the untreated group but they do not reflect the differences shown in Fig. 3. Rather, overall Hsp60 expression in the light treated group was more clustered and here it was less diffuse. Differences were clearer in the OPL and IPL than at other locations. No differences were seen in inner segments (data not shown).

4. Discussion

This study reveals a premature decline in retinal ATP in the *Cfh*$^{-/-}$ mouse as it ages and this is associated with changes in Hsp60 expression. The reduction in ATP is corrected and/or moderated by exposure to near infrared light, which is known to increase mitochondrial membrane potentials and COX expression along with ATP levels in aged mice (Begum et al., 2013; Gkotsi et al., 2014; Kokkinopoulos et al., 2013). These data reveal that mitochondrial dysfunction may be important in understanding this mouse model. The decline found here in mitochondrial function is established before development of the ocular phenotype in terms of inflammation and Aβ deposition and reduced retinal function identified at 12 months and may underpin disease development (Hoh Kam et al., 2013). If correct, inflammation and extracellular deposition that are key features of this mouse may be related to low cellular energy levels that restrict normal metabolic function.

Many factors drive aging, but the mitochondrial theory of aging has a degree of prominence. It argues that, with age mtDNA accumulates progressive mutations, reducing ATP production and increasing reactive oxygen species. This change in the balance of mitochondrial function is associated with chronic inflammation that leads to cell loss and tissue degradation (Archer, 2013; Harman, 1972; Lane, 2005; Lopez-Otin et al., 2013). Although this is a relatively simplistic interpretation, elements of the theory retain acceptance (Lopez-Otin et al., 2013). There is also an association between the pace of these events and metabolic rate at both the level of the organism (Speakman, 2005) and the tissue type (Wang et al., 2010). As the outer retina has the highest metabolic rate in the body (Yu and Cringle, 2001), it is not surprising that it becomes subject to progressive chronic inflammation aggravated by continued extension of life span. Hence, the incidence of AMD is increasing (Jonas, 2014).

Our ATP measurements are consistent with Gkotsi et al. (2014) who showed age-related decline in normal mouse retina and brain. However, we show that such patterns are different in *Cfh*$^{-/-}$ mice where decline is premature. The *Cfh*$^{-/-}$ mouse has been proposed as an AMD model (Coffey et al., 2007), and although it shares similarities of genotype and potential immune vulnerability with around 50% of AMD cases (Zipfel et al., 2010), reservation must be maintained regarding its use as a model of this disease, as rodents lack any significant central retinal specialization or macular (Cunea et al., 2014; Jeon et al., 1998) and have very different patterns of immune vulnerability compared with humans (Radermacher and Haouzi, 2013; Seok et al., 2013). Significant differences in immune vulnerability even occur between rats and mice (Zolfaghari et al., 2013). These differences are major challenges to the use of mice in this research area. But this mouse does display advanced patterns of retinal aging compared with C57BL/6 animals with significant thickening of Bruch's membrane, premature photoreceptor loss, heavy Aβ accumulation (Hoh Kam et al., 2013) and elevated retinal and choroidal inflammation (Catchpole et al., 2013; Coffey et al., 2007; Lundh von Leithner et al., 2009). But, in mice, these events are pan retinal rather than present only in central regions.

Consistent with high-retinal metabolic demand, there was a 5-fold difference between retinal and brain ATP levels, although in both tissues this declined at similar rates with age. The accelerated retinal decline in ATP in the *Cfh*$^{-/-}$ retina was associated subsequently with changes in patterns of Hsp60 expression. Hsp60 is upregulated in stress and is a chaperone that plays a role in the regulation of protein folding (Ostermann et al., 1989; Saibil, 2013). Although Hsp60 label remained diffuse at 8 months in C57BL/6 mice, in *Cfh*$^{-/-}$ animals it was punctate on morphological forms similar to individual mitochondria. This was marked in the plexiform layers, but difficult to discern in the inner segments where mitochondrial concentration is very high. Hsp60 is also involved in the replication and transmission of mtDNA (Brocchieri and Karlin, 2000; Cappello et al., 2008; Kaufman et al., 2003) as when it is mutated there are mtDNA transmission defects (Kaufman et al., 2003). Hence, improved mtDNA transmission is likely to be related to improved ATP production. Interestingly, Hsp60 also has the ability to activate monocytes and macrophages (Hansen et al., 2003), which show significant reductions when exposed to 670-nm light in aged mouse retinae (Begum et al., 2013; Kokkinopoulos et al., 2013).

There is evidence that declining ATP may be the precipitating factor driving outer retinal inflammation and cell loss. Retinal inflammation in C57BL/6 mice appears at approximately 12 months, which is also around when Aβ is first seen on Bruch's membrane (Catchpole et al., 2013; Lundh von Leithner et al., 2009). In *Cfh*$^{-/-}$ mice, these events occur earlier with significant inflammation present at 6–8 months, which is also when Aβ deposition occurs on Bruch's membrane (Catchpole et al., 2013; Kokkinopoulos et al., 2013; Lundh von Leithner et al., 2009). Hence, ATP decline occurs before the establishment of pathology in both genotypes. Rod photoreceptors loss appears after inflammation is established occurring largely in the second year in C57BL/6 mice and rats (Cunea and Jeffery, 2007; Fox and Rubinstein, 1989; Kolesnikov et al., 2010) but is already present at the end of the first year in *Cfh*$^{-/-}$ mice (Hoh Kam et al., 2013).

The data presented for changes in Hsp60 expression are consistent with those showing reduced ATP and reflect increased inflammation in these mice as they age along with thickening of Bruch's membrane that may drive retinal hypoxia (Hoh Kam et al., 2013). By 8 months, there are differences between the 2 groups of mice, with Hsp60 more focused in the *Cfh*$^{-/-}$ animals, although total levels did not differ between the 2 groups of mice.

Near infrared light is absorbed by COX (Szundi et al., 2001; Wilson and Greenwood, 1970) and upregulates its protein and RNA expression in the retina (Begum et al., 2013). In old C57BL/6 mice, it increases mitochondrial membrane potentials that have declined with age. This occurs following brief repeated exposures. This is associated with significant reductions in age-related inflammatory markers including reductions in macrophages and C3 and tumor necrosis factor alpha expression (Begum et al., 2013; Kokkinopoulos et al., 2013). It also increases retinal ATP in old C57BL/6 mice, similar to that presented here for *Cfh*$^{-/-}$ animals (Gkotsi et al., 2014). In *Cfh*$^{-/-}$ mice 670 nm has also been shown to reduce age-related inflammation (Begum et al., 2013), although no measurements of ATP were made. The beneficial impact of 670 nm has been found with diverse-induced pathologies to the eye and brain (Fitzgerald et al., 2013). Interventions have shown strong positive effects when pathology relates to impaired mitochondrial function, as in models of Parkinson's disease induced by 1-methyl-4-phenyl-1,2,3,6-tetrahydropyridine (Keane et al., 2011; Moro et al., 2014). Also, as the mitochondrial theory of aging argues that declining mitochondrial function is a significant driver of aging, it may be predicted that improvements here should increase life span. Although this is not known in mice it has been demonstrated in flies where 670 nm exposure not only increased ATP and reduced inflammation but also extended life span and improved aged mobility (Begum et al., 2015).

Given the influence of near infrared light, changes in Hsp60 may be expected after exposure, but the impact here was largely qualitative. Changes were restricted to label becoming focused on what were probably mitochondria. It is possible that clustering in the OPL layer may relate to cone terminals as they have higher mitochondrial density (Stone et al., 2008). Cones account for only around 3% of mouse photoreceptors (Carter-Dawson and LaVail, 1979) and cluster spacing may reflect this. Similar patterns are seen for COX IV staining when combined with that for cone opsins (Johnson et al., 2007. See Fig. 3). Although age-related patterns of photoreceptor loss have focused on rods (Curcio, 2001; Hoh Kam et al., 2013; Kolesnikov et al., 2010), it has been shown that mouse cones are lost before rods in peripheral long and/or medium wave sensitive cells in both C57BL/6 and *Cfh*$^{-/-}$ mice. But again, it is more marked in *Cfh*$^{-/-}$ (Cunea et al., 2014). In light of this, it may be of interest that physiological recordings from AMD patients, find signs of early disease in cone function (Binns and Margrain, 2007).

We reveal premature changes in mitochondrial function in *Cfh*$^{-/-}$ potentially placing mitochondria in a key position in phenotype development. As mitochondria provide energy for cellular metabolism they are widely implicated in diseases, particularly in the nervous system (Archer, 2013; Chen and Chan, 2009; Schon and Manfredi, 2003). High energy demand may be disadvantageous as life span extends as it is associated with rapid aging (Speakman, 2005; Wang et al., 2010). As human, life span throughout evolution has been much shorter than it is today (Caspari and Lee, 2004); extending it further may be associated with an increase in mitochondrial diseases in energy demanding tissues (Archer, 2013).

Disclosure statement

The authors declare no conflict of interest. All animals were used with University College London ethical committee approval and under a Home Office animal project license. All animal procedures conformed to the United Kingdom Animals Scientific Procedures Act 1986.

Acknowledgements

This research was supported by The Rosetrees Trust. Karin C. Calaza was a research fellow from CAPES (Proc. N° 18134/12-2).

References

Archer, S.L., 2013. Mitochondrial dynamics-mitochondrial fission and fusion in human diseases. N. Engl. J. Med. 369, 2236–2251.
AREDS2 Research Group, Chew, E.Y., Clemons, T., SanGiovanni, J.P., Danis, R., Domalpally, A., McBee, W., Sperduto, R., Ferris, F.L., 2012. The Age-Related Eye Disease Study 2 (AREDS2): study design and baseline characteristics (AREDS2 report number 1). Ophthalmology 119, 2282–2289.
Balaban, R.S., Nemoto, S., Finkel, T., 2005. Mitochondria, oxidants, and aging. Cell 120, 483–495.
Barot, M., Gokulgandhi, M.R., Mitra, A.K., 2011. Mitochondrial dysfunction in retinal diseases. Curr. Eye Res. 36, 1069–1077.
Begum, R., Calaza, K., Hoh Kam, J., Salt, T.E., Hogg, C., Jeffery, G., 2015. Near infrared light increases ATP, extends lifespan and improves mobility in aged Drosophila melangaster. Biol. Lett. 11, 1–4.
Begum, R., Powner, M.B., Hudson, N., Hogg, C., Jeffery, G., 2013. Treatment with 670 nm light up regulates cytochrome C oxidase expression and reduces inflammation in an age-related macular degeneration model. PLoS One 8, e57828.
Binns, A.M., Margrain, T.H., 2007. Evaluating retinal function in age-related maculopathy with the ERG photostress test. Invest. Ophthalmol. Vis. Sci. 48, 2806–2813.
Brocchieri, L., Karlin, S., 2000. Conservation among HSP60 sequences in relation to structure, function, and evolution. Protein Sci. 9, 476–486.
Cappello, F., Conway de Macario, E., Marasa, L., Zummo, G., Macario, A.J., 2008. Hsp60 expression, new locations, functions and perspectives for cancer diagnosis and therapy. Cancer Biol. Ther. 7, 801–809.
Carter-Dawson, L.D., LaVail, M.M., 1979. Rods and cones in the mouse retina. I. Structural analysis using light and electron microscopy. J. Comp. Neurol. 188, 245–262.
Caspari, R., Lee, S.H., 2004. Older age becomes common late in human evolution. Proc. Natl. Acad. Sci. U. S. A. 101, 10895–10900.
Catchpole, I., Germaschewski, V., Hoh Kam, J., Lundh von Leithner, P., Ford, S., Gough, G., Adamson, P., Overend, P., Hilpert, J., Lopez, F.J., Ng, Y.S., Coffey, P., Jeffery, G., 2013. Systemic administration of Abeta mAb reduces retinal deposition of Abeta and activated complement C3 in age-related macular degeneration mouse model. PLoS One 8, e65518.
Chen, H., Chan, D.C., 2009. Mitochondrial dynamics–fusion, fission, movement, and mitophagy–in neurodegenerative diseases. Hum. Mol. Genet. 18, R169–R176.
Coffey, P.J., Gias, C., McDermott, C.J., Lundh, P., Pickering, M.C., Sethi, C., Bird, A., Fitzke, F.W., Maass, A., Chen, L.L., Holder, G.E., Luthert, P.J., Salt, T.E., Moss, S.E., Greenwood, J., 2007. Complement factor H deficiency in aged mice causes retinal abnormalities and visual dysfunction. Proc. Natl. Acad. Sci. U. S. A. 104, 16651–16656.
Cunea, A., Jeffery, G., 2007. The ageing photoreceptor. Vis. Neurosci. 24, 151–155.
Cunea, A., Powner, M.B., Jeffery, G., 2014. Death by color: differential cone loss in the aging mouse retina. Neurobiol. Aging 35, 2584–2591.
Curcio, C.A., 2001. Photoreceptor topography in ageing and age-related maculopathy. Eye 15 (Pt 3), 376–383.
Edwards, A.O., Ritter 3rd, R., Abel, K.J., Manning, A., Panhuysen, C., Farrer, L.A., 2005. Complement factor H polymorphism and age-related macular degeneration. Science 308, 421–424.
Fitzgerald, M., Hodgetts, S., Van Den Heuvel, C., Natoli, R., Hart, N.S., Valter, K., Harvey, A.R., Vink, R., Provis, J., Dunlop, S.A., 2013. Red/near-infrared irradiation therapy for treatment of central nervous system injuries and disorders. Rev. Neurosci. 24, 205–226.
Fox, D.A., Rubinstein, S.D., 1989. Age-related changes in retinal sensitivity, rhodopsin content and rod outer segment length in hooded rats following low-level lead exposure during development. Exp. Eye Res. 48, 237–249.
Gkotsi, D., Begum, R., Salt, T., Lascaratos, G., Hogg, C., Chau, K.Y., Schapira, A.H., Jeffery, G., 2014. Recharging mitochondrial batteries in old eyes. Near infra-red increases ATP. Exp. Eye Res. 122, 50–53.
Griffiths, D.E., Wharton, D.C., 1961. Purification and properties of cytochrome oxidase. Biochem. Biophys. Res. Commun. 4, 151–155.
Haines, J.L., Hauser, M.A., Schmidt, S., Scott, W.K., Olson, L.M., Gallins, P., Spencer, K.L., Kwan, S.Y., Noureddine, M., Gilbert, J.R., Schnetz-Boutaud, N., Agarwal, A., Postel, E.A., Pericak-Vance, M.A., 2005. Complement factor H variant increases the risk of age-related macular degeneration. Science 308, 419–421.
Hansen, J.J., Bross, P., Westergaard, M., Nielsen, M.N., Eiberg, H., Borglum, A.D., Mogensen, J., Kristiansen, K., Bolund, L., Gregersen, N., 2003. Genomic structure of the human mitochondrial chaperonin genes: HSP60 and HSP10 are localised head to head on chromosome 2 separated by a bidirectional promoter. Hum. Genet. 112, 71–77.
Harman, D., 1972. The biologic clock: the mitochondria? J. Am. Geriatr. Soc. 20, 145–147.
Hoh Kam, J., Lenassi, E., Jeffery, G., 2010. Viewing ageing eyes: diverse sites of amyloid beta accumulation in the ageing mouse retina and the up-regulation of macrophages. PLoS One 5, 1–12.
Hoh Kam, J., Lenassi, E., Malik, T.H., Pickering, M.C., Jeffery, G., 2013. Complement component C3 plays a critical role in protecting the aging retina in a murine model of age-related macular degeneration. Am. J. Pathol. 183, 480–492.
Jarrett, S.G., Lin, H., Godley, B.F., Boulton, M.E., 2008. Mitochondrial DNA damage and its potential role in retinal degeneration. Prog. Retin. Eye Res. 27, 596–607.
Jeon, C.J., Strettoi, E., Masland, R.H., 1998. The major cell populations of the mouse retina. J. Neurosci. 18, 8936–8946.
Johnson, J.E., Perkins, G.A., Giddabasappa, A., Chaney, S., Xiao, W., White, A.D., Brown, J.M., Waggoner, J., Ellisman, M.H., Fox, D.A., 2007. Spatiotemperal regulation of ATP and Ca^{2+} dynamics in vertebrate rod and cone ribbon synapses. Mol. Vis. 13, 887–919.
Jonas, J.B., 2014. Global prevalence of age-related macular degeneration. Lancet Glob. Health 2, e65–e66.
Kaufman, B.A., Kolesar, J.E., Perlman, P.S., Butow, R.A., 2003. A function for the mitochondrial chaperonin Hsp60 in the structure and transmission of mitochondrial DNA nucleoids in Saccharomyces cerevisiae. J. Cell Biol. 163, 457–461.
Keane, P.C., Kurzawa, M., Blain, P.G., Morris, C.M., 2011. Mitochondrial dysfunction in Parkinson's disease. Parkinson's Dis. 2011, 716871.
Kokkinopoulos, I., Colman, A., Hogg, C., Heckenlively, J., Jeffery, G., 2013. Age-related retinal inflammation is reduced by 670 nm light via increased mitochondrial membrane potential. Neurobiol. Aging 34, 602–609.
Kolesnikov, A.V., Fan, J., Crouch, R.K., Kefalov, V.J., 2010. Age-related deterioration of rod vision in mice. J. Neurosci. 30, 11222–11231.
Lane, N., 2005. Power, Sex, Suicide. Mitochondria and the Meaning of Life, New edition. Oxford University Press, Oxford.
Lopez-Otin, C., Blasco, M.A., Partridge, L., Serrano, M., Kroemer, G., 2013. The hallmarks of aging. Cell 153, 1194–1217.
Lundh von Leithner, P., Kam, J.H., Bainbridge, J., Catchpole, I., Gough, G., Coffey, P., Jeffery, G., 2009. Complement factor h is critical in the maintenance of retinal perfusion. Am. J. Pathol. 175, 412–421.
Moro, C., Massri, N.E., Torres, N., Ratel, D., De Jaeger, X., Chabrol, C., Perraut, F., Bourgerette, A., Berger, M., Purushothuman, S., Johnstone, D., Stone, J., Mitrofanis, J., Benabid, A.L., 2014. Photobiomodulation inside the brain: a novel method of applying near-infrared light intracranially and its impact on dopaminergic cell survival in MPTP-treated mice. J. Neurosurg. 120, 670–683.
Nordgaard, C.L., Karunadharma, P.P., Feng, X., Olsen, T.W., Ferrington, D.A., 2008. Mitochondrial proteomics of the retinal pigment epithelium at progressive

stages of age-related macular degeneration. Invest. Ophthalmol. Vis. Sci. 49, 2848–2855.
Ostermann, J., Horwich, A.L., Neupert, W., Hartl, F.U., 1989. Protein folding in mitochondria requires complex formation with hsp60 and ATP hydrolysis. Nature 341, 125–130.
Radermacher, P., Haouzi, P., 2013. A mouse is not a rat is not a man: species-specific metabolic responses to sepsis - a nail in the coffin of murine models for critical care research? Intensive Care Med. Exp. 1, 7.
Saibil, H., 2013. Chaperone machines for protein folding, unfolding and disaggregation. Nat. Rev. Mol. Cell Biol. 14, 630–642.
Schon, E.A., Manfredi, G., 2003. Neuronal degeneration and mitochondrial dysfunction. J. Clin. Invest. 111, 303–312.
Seok, J., Warren, H.S., Cuenca, A.G., Mindrinos, M.N., Baker, H.V., Xu, W., Richards, D.R., McDonald-Smith, G.P., Gao, H., Hennessy, L., Finnerty, C.C., Lopez, C.M., Honari, S., Moore, E.E., Minei, J.P., Cuschieri, J., Bankey, P.E., Johnson, J.L., Sperry, J., Nathens, A.B., Billiar, T.R., West, M.A., Jeschke, M.G., Klein, M.B., Gamelli, R.L., Gibran, N.S., Brownstein, B.H., Miller-Graziano, C., Calvano, S.E., Mason, P.H., Cobb, J.P., Rahme, L.G., Lowry, S.F., Maier, R.V., Moldawer, L.L., Herndon, D.N., Davis, R.W., Xiao, W., Tompkins, R.G., Inflammation, Host Response to Injury, L.S.C.R.P, 2013. Genomic responses in mouse models poorly mimic human inflammatory diseases. Proc. Natl. Acad. Sci. U. S. A. 110, 3507–3512.
Speakman, J.R., 2005. Body size, energy metabolism and lifespan. J. Exp. Biol. 208 (Pt 9), 1717–1730.
Stone, J., van Driel, D., Valter, K., Rees, S., Provis, J., 2008. The locations of mitochondria in mammalian photoreceptors: relation to retinal vasculature. Brain Res. 1189, 58–69.
Szundi, I., Liao, G.L., Einarsdottir, O., 2001. Near-infrared time-resolved optical absorption studies of the reaction of fully reduced cytochrome c oxidase with dioxygen. Biochemistry 40, 2332–2339.
Udar, N., Atilano, S.R., Memarzadeh, M., Boyer, D.S., Chwa, M., Lu, S., Maguen, B., Langberg, J., Coskun, P., Wallace, D.C., Nesburn, A.B., Khatibi, N., Hertzog, D., Le, K., Hwang, D., Kenney, M.C., 2009. Mitochondrial DNA haplogroups associated with age-related macular degeneration. Invest. Ophthalmol. Vis. Sci. 50, 2966–2974.
Wang, Z., Ying, Z., Bosy-Westphal, A., Zhang, J., Schautz, B., Later, W., Heymsfield, S.B., Muller, M.J., 2010. Specific metabolic rates of major organs and tissues across adulthood: evaluation by mechanistic model of resting energy expenditure. Am. J. Clin. Nutr. 92, 1369–1377.
Wilson, M., Greenwood, C., 1970. The long-wavelength absorption band of cytochrome c oxidase. Biochem. J. 116, 17P–18P.
Yu, D.Y., Cringle, S.J., 2001. Oxygen distribution and consumption within the retina in vascularised and avascular retinas and in animal models of retinal disease. Prog. Retin. Eye Res. 20, 175–208.
Zipfel, P.F., Lauer, N., Skerka, C., 2010. The role of complement in AMD. Adv. Exp. Med. Biol. 703, 9–24.
Zolfaghari, P., Pinto, B., Dyson, A., Singer, M., 2013. The metabolic phenotype of rodent sepsis: cause for concern? Intensive Care Med. Exp. 1, 6.